

An Investigation into the Glass Transition Temperature of Vapor Phase Infiltrated Organic-Inorganic Hybrid Materials

*Undergraduate Thesis by James Bamford
School of Materials Science and Engineering*

Faculty Member #1

Printed: Mark D. Losego

Signature: _____

Faculty Member #2

Printed: Will R. Gutekunst

Signature: _____

Table of Contents

Abstract	4
Introduction.....	5
Literature Review	7
Methodology.....	10
<i>PS-r-PHEMA Synthesis and Characterization</i>	10
<i>Copolymer Thin Film Preparation</i>	11
<i>Vapor Phase Infiltration</i>	12
<i>Spectroscopic Ellipsometry & Measurements of Glass Transition Temperature</i>	13
<i>Dissolution in Chloroform</i>	14
<i>Fourier-Transform Infrared Spectroscopy (FTIR)</i>	14
<i>Second Ion Mass Spectroscopy (SIMS)</i>	15
Results and Discussion	16
<i>Alumina Uptake in Copolymer Films</i>	16
<i>Thermal Expansion and Glass Transition Temperature</i>	18
<i>Chemical Stability and Crosslinker Swelling</i>	21
<i>Chemical Bonding between Alumina and PS-r-PHEMA</i>	22
Conclusion	25
References.....	26

Appendix30

Abstract

Glass transition temperature (T_g) is a fundamental property of a polymer that defines its upper service temperature for structural applications and is reflective of its physicochemical features. We are interested in how vapor phase infiltration (VPI), which infuses polymers with inorganic species to create hybrid materials, affects the glass transition temperature of a material. We examine Al_2O_3 VPI into poly(styrene-co-2-hydroxyethyl methacrylate) (PS-*r*-PHEMA) using trimethylaluminum (TMA) and water precursors. Our VPI precursors are selected to be unreactive towards the styrene monomer units and highly reactive towards the HEMA monomer units. Experiments were conducted on PS-*r*-PHEMA thin films (200 nm) spun-cast onto silicon wafers and infiltrated at 100°C with 4 hr. exposure times. Copolymers with varying fractions of HEMA units were investigated, from 0 mole % to 20.2 mole % HEMA. Volumetric swelling of the films after VPI and aluminum oxide film thicknesses after pyrolysis both confirmed higher metal oxide loading with higher fraction HEMA units. T_g was measured using a spectroscopic ellipsometer with a heating unit. We find that the glass transition temperature increases significantly with metal oxide loading. Copolymers with 0.0%, 3.0%, 7.7%, 11.5%, and 20.2% HEMA units experienced 6°C, 8°C, 22°C, 37°C, and 46°C increases in T_g respectively. Changes in T_g at low HEMA composition fit the Fox-Loshaek model for crosslinking phenomena which, along with a dissolution study on these materials, suggests that VPI alumina crosslinks PS-*r*-PHEMA. We conclude that VPI may be useful as a crosslinking process for designing the thermophysical and thermochemical properties of polymer thin films, fibers, and fabrics.

Introduction

Vapor phase infiltration (VPI) is a material hybridization process that infuses polymers with metal oxide compounds. During VPI, a polymer substrate is exposed to a vaporous metalorganic precursor that diffuses into the porous polymer network and chemically binds to the internal polymer chains. How this impacts polymer properties largely depends on VPI temperature, pressure, timing, and materials selected (the polymer substrate and the metalorganic precursor). These variables can influence the amount of metal oxide infiltrated, as well as the nature of polymer-metal interactions; metal oxide networks may kinetically entangle or form chemically bound crosslinks between polymer chains. Potential applications of VPI-created hybrid materials include oil sorbents, photovoltaics, lithography, antireflective coatings, and membranes¹⁶⁻²⁰.

In addition to studying recently discovered VPI material properties, understanding the molecular transformation in this process enables the prediction and discovery of entirely new properties. The thermophysical properties of VPI-created hybrid materials have not been extensively explored. For example, no changes in glass transition temperature (T_g) have been reported to the best of our knowledge. T_g is a fundamental property of a polymer that defines its upper service temperature in many applications and is reflective of its physiochemical features. This temperature marks the transition from a glassy state of low chain mobility to a rubbery state of high chain mobility in solid amorphous polymers. Meanwhile, crosslinking (the chemical binding of multiple polymer molecules to each other) is a structural transformation at the molecular scale that drastically reduces polymer chain mobility, thereby increasing T_g ^{1,2,6,12}. In applications where polymers must function in their glassy form, crosslinking becomes a useful

mechanism for increasing a product's upper service temperature. Studying VPI through the lens of these two phenomena (T_g and crosslinks), we expect VPI crosslinks to have a significant impact on polymer glass transition.

This investigation establishes a relationship between vapor phase infiltration and polymer glass transition temperature. We use poly(styrene-*r*-hydroxyethyl methacrylate) (PS-*r*-PHEMA) copolymers with varying compositions to control metal oxide loading. In this material system, TMA most likely reacts with the hydroxyl groups in HEMA; polymers with higher concentration HEMA monomer units therefore bind more alumina to their chains during VPI. In this manuscript, we measure thicknesses of heated polymer films in order to understand the relationship between VPI treatment and hybrid material T_g .

Literature Review

In order to study vapor phase infiltration through the lens of chemical crosslinking and glass transition, these two phenomena must first be understood in their own right. Crosslinks are chemical reactions between polymers (i.e. long chain molecules) that bind these chains together, significantly impacting polymer properties. VPI involves the infusion of solid polymer chain networks (i.e. plastics and fibers) with gaseous metallic compounds that are capable of crosslinking these polymer chains. Many impacts of VPI processing on polymer properties have been connected to possible crosslinking mechanisms. However, impacts on a particularly significant thermal property – polymer glass transition temperature (T_g) – have yet to be explored. Accordingly, this literature review first addresses the relationship between polymer T_g and crosslinking, followed by the relationship between VPI crosslinking and polymer properties more broadly, in order to emphasize this current gap in the VPI literature.

The impacts of polymer crosslinking on T_g have been well established through half a century of research. In 1964, DiMarzio proposed a simplified model that relates relative changes in T_g with polymer crosslinks, restated here²:

$$\frac{T(X)-T(0)}{T(0)} = \frac{KX}{1-KX} \quad (1)$$

Where $T(X)$ is the glass transition temperature of a polymer with crosslinking density, X (i.e. the mole fraction of crosslinked monomer units in a chain). K is a material constant. The earliest version of this equation was proposed in 1950 by Thomas Fox and Paul Flory. Glass transition is a second order phase transformation that marks the change upon heating from an amorphous solid polymer with reduced chain mobility (i.e. glassy mechanical properties) to a polymer with

increased chain mobility (rubbery / ductile mechanical properties). Chain mobility in crosslinked polymers is significantly reduced; accordingly, T_g increases with crosslinking density.

Over the years, this model has been both experimentally and theoretically supported by new studies, with modifications^{1,12}. Stutz et al. in 1990 considered how polymer end groups, molecular weight, and branching complicate this relationship, specifically by impacting the material constant K ¹². Many polymer systems studied during VPI crosslinking can be modelled by a version of equation 1 which considers the ideal case of large molecular weight (negating the effects of chain end groups) and post-synthesis processing of linear polymers (such as VPI). In this version, K is only dependent on the mobility of the actual crosslinking unit, which in the case of VPI metallic crosslinkers may be considered immobile. This importance on crosslinker selection is also emphasized by Bandzierz et al. who related T_g shifts to crosslinker size, structure, and chemistry in 2016¹.

Crosslinking mechanisms vary widely – especially between post-synthesis and through-synthesis techniques. In this context, vapor phase infiltration arises as a relatively new approach. During VPI, gaseous metalorganic compounds (precursors) diffuse into porous polymer chain networks (substrates), at which point the precursor may react with certain functional groups along the polymer chains. A commonly studied VPI material system is polymethyl methacrylate (PMMA) substrate and trimethyl aluminum (TMA) precursor^{5,7,9,13}. Hill et al. propose that aluminum oxide becomes chemically bound to PMMA via a pericyclic reaction between TMA and PMMA's carboxyl groups⁵. McGuinness et al. propose that the aluminum oxide may then (a) permanently bind to multiple polymer chains (forming crosslinks), (b) remain singly bound as pendant groups, or (c) detach from the chain to form kinetically entrapped metal oxide⁹.

Aluminum oxide formation has also been proposed as the resulting reaction between TMA and polymer hydroxyl groups, as studied with cellulose fibers and density functional theory (DFT)^{3,15}. In this manner, VPI cannot be considered exclusively a crosslinking mechanism. The exact nature of structural transformations that occur during VPI is dependent on processing conditions and materials selected.

Nonetheless, many impacts of VPI processing on polymer properties are similar to those of conventional crosslinking techniques. In particular, mechanical strength and chemical stability have both been shown to improve as a result of VPI. Leng et al. and Waldman et al. are two recent literature reviews that cover the impacts and applications of VPI and SIS (sequential infiltration synthesis, a similar process) respectively^{7,13}. Elastic modulus and tensile strength have both been found to increase in certain material systems as a result of VPI metal crosslinks that stiffen the polymer chains. Similarly, these crosslinks also decrease polymer solubility by replacing the intermolecular forces holding chains together with organometallic bonds.

Finally, it's crucial to note that while many properties of VPI material hybrids have been studied, glass transition temperature so far remains unreported to the best of our knowledge. At the same time, the impacts of crosslinking on T_g have been extensively studied, so one might expect a similar effect from VPI processing. We therefore propose to investigate of this exact relationship – VPI crosslinks and their effect on polymer T_g – in order to (a) better understand the extent to which VPI can be considered a crosslinking process and (b) promote the usage of VPI processing in new applications.

Methodology

PS-*r*-PHEMA copolymers with varying reactivities to TMA were synthesized to understand the effects of VPI as a function of TMA loading. In other words, copolymers synthesized with high concentration HEMA units that are highly reactive with TMA were designed to uptake more alumina than copolymers synthesized with low concentration. Copolymers were spin-coated into films so that they could be fully vapor phase infiltrated within a reasonable time frame (14 hours). During VPI, copolymer films underwent TMA exposure, nitrogen purges, and water exposure to ensure formation of alumina within the films. Films were characterized with ellipsometry in order to quantify alumina uptake and changes in T_g . In separate experiments, films were dissolved in chloroform or characterized with FTIR in order to understand the chemical interactions between alumina and PS-*r*-PHEMA. SIMS was also conducted to ensure full infiltration of the films.

*PS-*r*-PHEMA Synthesis and Characterization*

All polymers were synthesized by a collaborating lab group. In order to form PS-*r*-PHEMA copolymers, they combined HEMA and styrene via 2,2'-Azobisisobutyronitrile (AIBN) free radicalization in dry dimethylformamide (DMF) at 60°C for 16 hr. Copolymer composition was controlled by monomer feed ratio between styrene and HEMA. Copolymer precipitates were analyzed via ^1H NMR and GPC to confirm composition, molecular weight (M_n), and polydispersity (\mathcal{D}). These properties of the provided copolymers are summarized in Table 1.

mol.% HEMA	M_n (g/mol)	\bar{D}
0.0 %	63.6 k	1.67
3.0 %	65.8 k	1.65
7.7 %	67.0 k	1.69
11.5 %	69.0 k	1.72
20.2 %	93.4 k	1.57

Copolymer Thin Film Preparation

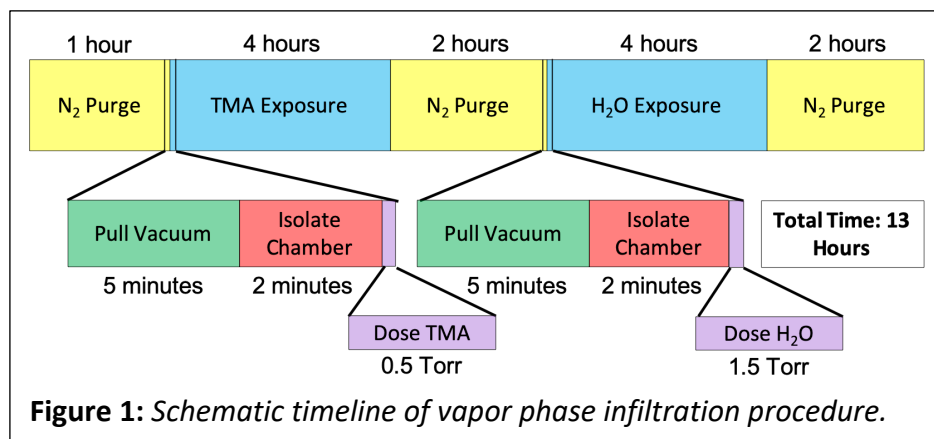
Polymer films were prepared via spin-coating from solution. Film thickness was chosen to (1) be sufficiently thick to avoid effects on T_g due to interactions with the substrate or free surface and (2) be sufficiently thin to be fully infiltrated via VPI within a reasonable amount of time. We find that a thickness of 200 nm met both of these criteria for our PS-*r*-PHEMA thin films.

To achieve this thickness, each copolymer was dissolved in chloroform at a ratio of 2 wt% polymer content. Pure polystyrene was dissolved in toluene at 5 wt%. Solutions stirred for at least 24 hr. and sat at rest for at least another 24 hr. letting any contaminants settle. Silicon wafers cut into 1 x 1 in² tiles were plasma cleaned for 1 min in an 18 W RF PDC-001-HP Plasma Cleaner to remove organic contaminants and surface hydroxyl groups. Tiles were then spun cast at 3000 rpm for 60 s (SCS 6800 spin coater). At about 5 s into the spin cycle, about 1 mL of polymer solution was dropped onto the spinning silicon wafer. After spin-coating, polymer thin films were annealed and dried on a hot plate at 150°C for at least 1 hr.

Vapor Phase Infiltration

PS-*r*-PHEMA thin films were vapor-phase-infiltrated according to the timeline in Fig. 1 using a custom-designed VPI reactor at 100°C. The initial 1 hr purge (pulling vacuum and flowing nitrogen) at 1 torr removed water and other loosely held contaminants from the films and reaction chamber. After pulling pure vacuum for an additional 5 min and isolating the chamber for 2 min, TMA was dosed for 5 s (0.5 torr partial pressure), held in the chamber for 4 hr, and purged out over 2 hr. After another 5 min pump down and 2 min isolation, water was dosed (5 s, or 1.5 torr), held, and purged for the same time intervals as TMA.

VPI reaction parameters were selected based on a prior kinetics study conducted with PS-*r*-PHEA (HEA standing for hydroxyl ethyl acrylate), a chemically similar copolymer to PS-*r*-PHEMA. Swelling data in Fig. 6 indicates minimal volumetric changes in copolymer films between 1 min and 1000 min purge times, suggesting that most unbound TMA leaves the copolymer within the first min of nitrogen purging. 2 hr purges were chosen for PS-*r*-PHEMA studied in this investigation to minimize the presence of unbound alumina in the polymer. SIMS data in Fig. 8 confirms that most copolymers were fully infiltrated with our selected TMA hold time, 4 hr.



Spectroscopic Ellipsometry & Measurements of Glass Transition Temperature

Thin film thicknesses were measured using a J.A. Woollam alpha-SE Ellipsometer retrofitted with a silica gel heating pad. Thickness and refractive index (RI) analysis was done using CompleteEASE software. We designed a Cauchy model to represent the copolymer and VPI hybrid films, fitting A, B, and k Cauchy coefficients of refractive index in addition to thickness. This layer was stacked on top of a 1.7 nm layer of SiO₂.

Copolymer thickness and RI for copolymers were measured at 60°C (using the ellipsometer's hot plate) before and after vapor phase infiltration. These measurements were always taken within 0.5 hr. after 150°C heat treatments, to minimize water sorption onto the films, which might conflate thickness results. We measured the same spot on each film before and after VPI to the best of our ability, minimizing variation from heterogeneous spin-coating across the tile (i.e. films were thicker near the edges of tiles, so measurements were taken at the center).

Glass transition and coefficients of thermal expansion were determined by measuring copolymer thickness over a temperature ramp. Measurements were taken over 5°C intervals, holding the films at each temperature for approximately 10 s. Differences thermal expansivity and T_g behavior between films held for 10 s and 30 s were negligible, so 10 s holds appears to reach thermal equilibrium (Fig. 7). Films remained stationary during each temperature, such that the exact same spot on the film was continuously measured.

Polymer was removed from the hybrid material via 1 hr of plasma cleaning, and the remaining AlO₂ was sintered in a furnace at 700°C for 1 hr. Alumina thicknesses were measured via ellipsometry using a Cauchy model with fixed RI constants (RI fitting becomes unrealistic

below 50 nm). Mean Squared Error (MSE) of this data refers to the differences between measured and modelled values of “N,” “S,” and “C,” variables in the CompleteEASE software, which are related to the psi and delta directly measured during ellipsometry. See page 3-45 of the “CompleteEASE Software Manual,” for more information.

Dissolution in Chloroform

In a different experiment, 200nm VPI-treated PS-*r*-PHEMA films were dissolved in separate containers, each with 10 ml chloroform. Thin film thicknesses were measured before dissolution, and after 1, 3, 10, and 30 hr. in chloroform. After each dissolution interval, the films were removed from solution and held against Kimwipes to remove chloroform from the surface. Film thicknesses were then measured on an ellipsometer after no longer than 10 min outside of solution to capture any swelling phenomena in addition to film dissolution. Films were returned to their original solutions for continued exposure. After the 30-hr measurement, films were annealed at 150°C for 1-hr to remove any solvent or swelling and measured once more. This experiment was repeated for untreated copolymers, dissolving them for 1 hr.

Fourier-Transform Infrared Spectroscopy (FTIR)

FTIR spectra were measured using a Thermo Fisher Scientific Nicolet iS5 Spectrometer with an iD7 ATR and an AR-coated diamond crystal. Through OMNIC software, absorption spectra were collected with 2 cm⁻¹ resolution and 128 scans per copolymer. We drop-casted micron-thick copolymers on silica glass slides for FTIR to reduce noise on the spectra. As with spin-coated films, the drop-casted films were dried and annealed at 150°C on a hot plate, but for 3 hr. due to their

larger thickness. FTIR spectra were collected for each copolymer before and after vapor phase infiltration.

Second Ion Mass Spectroscopy (SIMS)

SIMS spectra of the 200 nm AlO_x -PS-*r*-PHEMA films were measured with an IONTOF 5-300 Time-of-Flight SIMS system. A 2 keV electron beam was focused onto a 150x150 μm square section of the VPI-treated 200 nm PS-*r*-PHEMA films, and a 50x50 μm section within this region was analyzed. The beams penetrated through polymer films and into their supporting silicon wafers after 300 s of exposure.

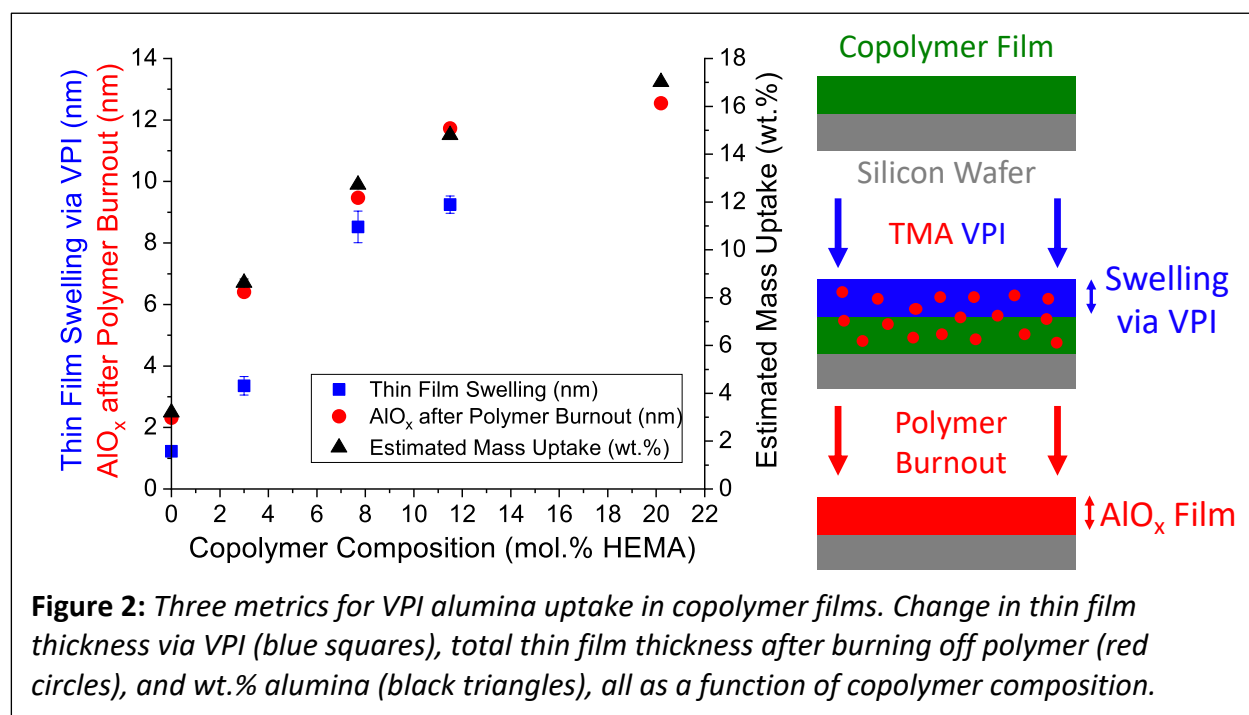
Results and Discussion

At low HEMA concentration in the copolymer, ellipsometry results show near-linear relationships between HEMA content, alumina uptake in terms of film volumetric swelling, and alumina uptake in terms of post-burnout film thickness. Furthermore, ellipsometry characterization with temperature ramps also show near-linearity between alumina uptake and increases in T_g . The dissolution study demonstrates chemical resistance in all infiltrated films except AlO_x -PS (i.e. no HEMA content). While FTIR results are inconclusive, the insolubility of AlO_x -PS-PHEMA films and the dramatic increases in T_g suggest that VPI-formed alumina crosslinks PS-*r*-PHEMA copolymer chains.

Alumina Uptake in Copolymer Films

Fig. 2 presents three ellipsometry-based metrics that relate VPI alumina loading with initial copolymer composition: copolymer film swelling, pyrolyzed alumina thickness, and alumina mass uptake. Film swelling is the change in total film thickness after VPI treatment. Polymer in the films were then burned out and the remaining alumina measured. Mass uptake is estimated with film thicknesses and material densities. Copolymer density is assumed to fit a linear interpolation between pure PS (1.05 g/ml, Sharp 1950) and PHEMA (1.15 ml, Sigma Aldrich). Amorphous alumina density of 3.2 g/ml is based on the literature value for atomic layer-deposited (ALD) alumina, a similar metalorganic treatment²¹. Polymer film thicknesses varied by 20 nm depending on copolymer composition, but this variation becomes normalized in the form of wt.% mass uptake.

All three metrics suggest a linear relationship between HEMA concentration and alumina uptake at low HEMA content (less than 20.2 mol.% HEMA). Film swelling ranged from 1.2 nm of growth in pure polystyrene (0% HEMA) to 14.4 nm in 20.2 mol.% HEMA. Similarly, alumina thickness ranged from 2.3 to 12.5 nm, and mass uptakes from 3.2 wt.% to 17.0%. Increasing alumina uptake with HEMA content supports the expectation that polymer-VPI reactivity can be controlled by the concentration of VPI-reactive sites. However, the alumina thickness and mass uptake for copolymer with 20.2 mol.% HEMA show diminishing returns at higher reactivity. SIMS data taken with these films suggests that a high concentration of AlO_x -PS-*r*-PHEMA bonds at film surfaces can prevent further TMA diffusion during VPI, limiting the total amount of alumina uptake possible (Fig. 8).



Ellipsometry measurements show refractive indices of PS-*r*-PHEMA films varied from 1.597 (pure PS) to 1.575 (Copolymer with 20.2% HEMA) \pm 0.001 at 500 nm (Fig. 9). This range agrees with literature values for pure polystyrene (1.604 at 500nm) and poly(hydroxyethyl

methacrylate) (1.51)^{22,23}. VPI treatment did not change refractive indices of these films by any more than 0.006 ± 0.002 (as seen with HEMA-8), suggesting that film volume is conserved. In other words, the additional volume measured after VPI is exclusively occupied by alumina; the density of the copolymer did not change.

After burning-off polymer from the VPI hybrids, the remaining films fitted moderately well (MSE less than 5) to a Cauchy model with a fixed refractive index at 1.660, which is a literature value for amorphous alumina²⁴. This agreement supports the expectation that trimethylaluminum produced alumina. Alumina film thicknesses exceed VPI film swelling at low HEMA concentration (less than 20.2 mol.% HEMA); the atomic density of amorphous alumina after pyrolysis may differ from its atomic density when bonded to polymer hydroxyls.

Thermal Expansion and Glass Transition Temperature

Temperature ramps and summary results from measuring thicknesses of untreated and VPI films at increasing temperatures are presented in Fig. 3. The slopes of these thickness-vs-temperature plots are thermal expansion coefficients for each film. Glass transition temperature (T_g) is graphically defined as the intersection between two thermal expansion coefficients – a glassy state below T_g and a rubbery state above. These lines were fitted with least squares regression, using all data points except those nearest T_g (some temperature ramps show a gradual transition between the two regimes of thermal expansion).

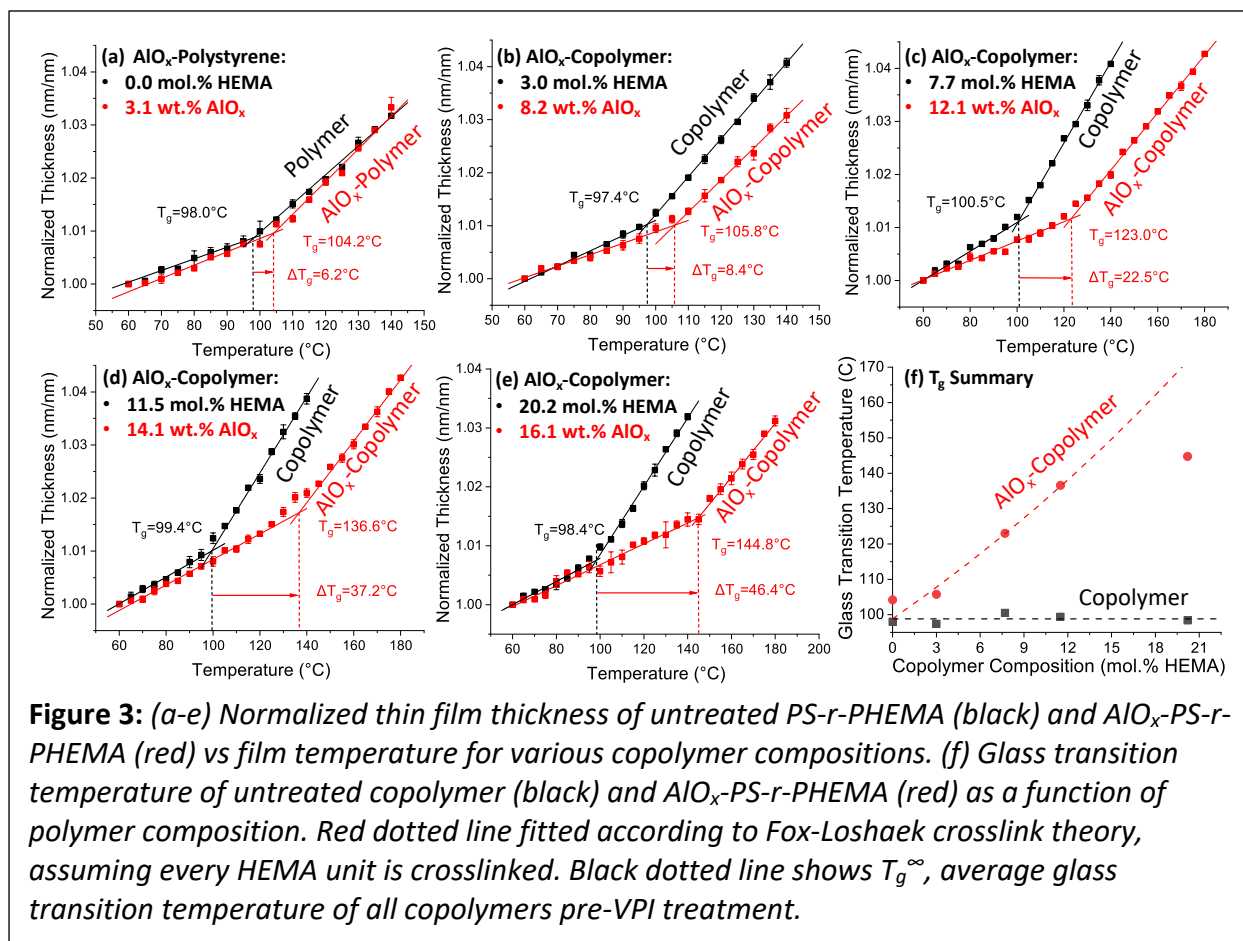
T_g has a remarkably clear relationship with VPI loading. Fig. 3f summarizes T_g values for untreated copolymers and AlO_x -PS-PHEMA hybrids. For untreated PS-*r*-PHEMA, T_g remains constant, within 3°C of the literature temperature for polystyrene films, 100°C⁸. After VPI

processing, T_g values for AlO_x -PS-PHEMA start at 104°C for AlO_x -PS (0 mol.% HEMA and 3.1 wt.% alumina) and increases up to 145°C for with the most infiltrated PS-PHEMA (20.2 mol.% HEMA, 16.1 wt.% alumina). Because HEMA content is related to alumina content at low HEMA compositions, this trend suggests that increasing vapor-phase-infiltrated alumina content in PS-*r*-PHEMA films suppresses chain mobility.

The positive correlation between alumina content and T_g suggests that VPI treatment suppresses polymer chain mobility. Alumina crosslinks between PS-PHEMA chains is a possible mechanism that would explain this relationship, which is further supported by the dissolution study (Fig. 4). The Fox-Loshaek equation (1) for T_g and crosslinking density X_c for large linear polymers crosslinked post-synthesis is fitted to the data in Fig. 3f and presented here¹²:

$$T_g = T_g^\infty \left[1 + K_2 \frac{X_c}{1-X_c} \right] \quad (1)$$

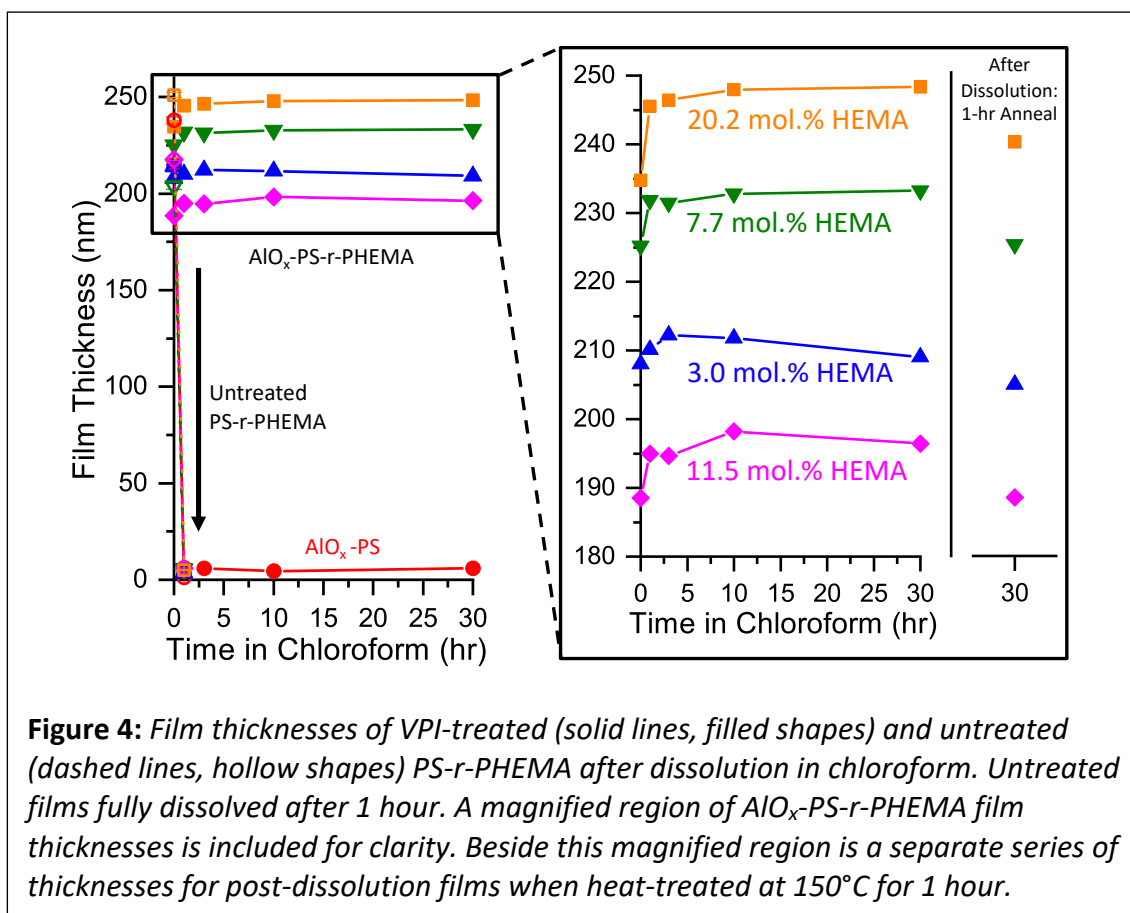
This model only accounts for changes in T_g as a function of crosslinks, so T_g^∞ is defined as the average glass transition temperature of all copolymers before VPI-treatment (98.8°C). Assuming all HEMA units are crosslinked, Pure polystyrene is excluded from this model because the change in glass transition observed there may occur from some other mechanism at the interfacial boundary where most alumina is located. Copolymer with 20.2 mol.% HEMA is excluded because it is not fully infiltrated. In fact, the theory that this polymer is partially infiltrated is supported by the observation that T_g for 20.2 mol.% HEMA VPI-treated polymer lies below the predicted Fox-Loshaek value for that composition.



Because the Fox-Loshak model takes a linear form at low crosslink density, K_2 can be thought of as the slope of T_g vs. X_c , or in other words, the extent to which a crosslinker reduces chain mobility. 2.9 is more than 3 times the K_2 values for conventional polymer crosslinkers, such as ethyleneglycoldimethacrylate with PMMA, divinylbenzene with PS, and Desmodur RF with polyurethane (Stutz 1990). As such, these changes in T_g present VPI not only as a unique processing technique for processing polymers, but one that may reduce polymer chain mobility more effectively than conventional crosslinker chemistries.

Chemical Stability and Crosslinker Swelling

Improved chemical stability and swelling behavior in the VPI-treated polymers further promote the possibility of alumina-based polymer crosslinking. Fig. 4 presents an ex-situ dissolution study with AlO_x -PS-*r*-PHEMA in chloroform. All untreated polymers dissolved within 1 hr. VPI infiltrated AlO_x -polystyrene thickness also drops from 200 nm to below 10 nm within the first hour in chloroform and remains there for the rest of the study. In contrast, none of the AlO_x -copolymer thicknesses dropped below their initial values, until heat-treated post-dissolution. Even then, no copolymer film dropped beneath 4 nm of its original thickness. Most of these films swelled in chloroform, up to a 13-nm increase of the original thickness for HEMA-20 before heat-treatment.



While a higher degree of crosslinking is known to reduce the extent of swelling, the opposite trend is apparent in the magnified region of Fig. 4. An increase in swelling due to less crosslinks might be negated by a reduction in film volume. In other words, the low-HEMA, low-alumina copolymers may be partially dissolving. It should be noted that the error bars for these thicknesses reflect one film per copolymer measured three times; more data would help clarify the extent of chemical stability and swelling in these metalorganic hybrids. Nonetheless, it is clearly evident that VPI treatment drastically improves polymer stability. Alumina crosslinks between PS-*r*-PHEMA chains are the most probable cause for this behavior.

Interestingly, 3 to 6 nm of untreated copolymer and AlO_x-PS films remain after dissolution. For AlO_x-PS, 4.8 nm of film remain after 30 hr. in the chloroform and 1 hr. at 150°C, whereas alumina only accounts for 2.2 nm after polystyrene burnout (Fig. 2). All the alumina for VPI-treated polystyrene was found in the interfacial region between film and silicon wafer, so the additional thickness might be a layer of polystyrene bound to this region through defects and alumina bonding. Post-dissolution thickness in untreated copolymers may be explained by hydrogen or covalent bonds between HEMA units and hydroxyls on the silicon surface. This conjecture is supported by the fact that only 1 nm of untreated PS remained after dissolution, compared to 3-6 nm for untreated copolymers.

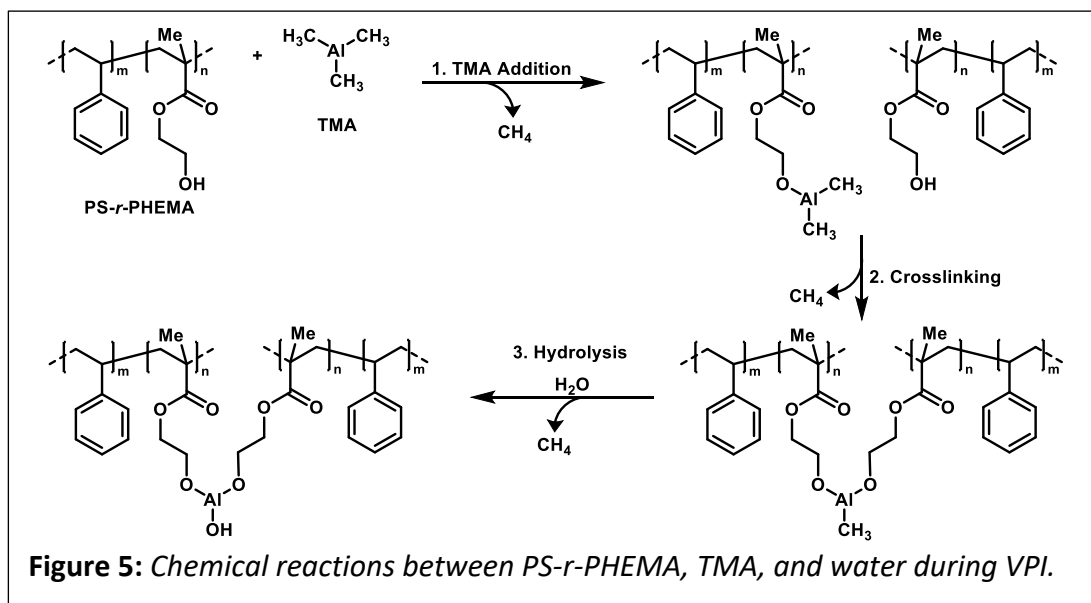
Chemical Bonding Between Alumina and PS-r-PHEMA

No clear conclusions can be made by comparing the FTIR spectra of copolymer and metalorganic hybrid films (Fig. 10). The intensity of each spectra for AlO_x-Copolymers (i.e. after VPI) is normalized to match the equivalent untreated copolymer (before VPI) peak at 2930 cm⁻¹,

which is not expected to change. This peak represents C-H bending in the methylene polymer backbone, which exists at a significant composition in all PS-*r*-PHEMA copolymers tested. All other peaks in the spectra can be matched to the aromatic bonds in styrene, the C=O, C-O, and O-H bonds in HEMA, and the Si-O bonds in the wafer. Peak-by-peak assignment is included in the Appendix.

Only one notable difference in FTIR spectra emerges from VPI treatment: a broadening and rightward shift of the hydroxyl stretch at from 3300 to 3500 cm^{-1} . This shift may reflect hydroxyls in a different chemical environment than the HEMA units, such as bound or unbound alumina. Alternatively, VPI treatment may have affected the hydrophobicity of the films, resulting in more or less water sorption. To minimize this effect, II FTIR was taken within 15 min after 1 hr heat treatments at 150°C.

Other than this shift, no FTIR peaks are noticeably formed, removed, amplified, or reduced as a result of vapor phase infiltration. Accordingly, these results suggest that alumina may be (a) chemically unbound to the copolymers, thereby showing no organic-inorganic bonds, (b) bound in a manner that does not appear on FTIR spectra, or (c) bound in a manner that does not change the stoichiometric proportions of chemical bonds. The exact mechanisms for chemical reaction between alumina, PS-*r*-PHEMA and water are beyond the scope of this investigation. In general, we believe that during TMA dosing and holding, TMA undergoes a substitution reaction with the hydroxyl groups in PS-*r*-PHEMA, binding aluminum to the polymer with a C-O-Al bond and releasing methane (Fig. 5). During the water dose-and-hold, hydroxyl bonds replace all remaining Al-methyl bonds, releasing more methane. By bonding to multiple chains during the first step, TMA may form crosslinks that significantly alter material properties.



Conclusion

PS-*r*-PHEMA copolymers were successfully synthesized via AIBN free-radical polymerization. 200 nm spun-cast copolymer films with up to 7.7 mol.% HEMA units were fully vapor-phase infiltrated with alumina at 100°C after 4 hr of TMA exposure. 11.5 and 20.2 mol.% HEMA films were partially infiltrated under similar conditions. Linearity between copolymer HEMA content, volumetric swelling after VPI, and film thickness after pyrolysis confirms that the concentration of alumina in VPI material hybrids is tunable by designing selectively reactive polymers. TMA diffusion through more reactive polymers (in this case, higher concentration HEMA units) appears to be limited by dense alumina formation at the substrate surface. Chemical stability and volumetric swelling in VPI-treated copolymers during dissolution studies both suggest that alumina crosslinks PS-*r*-PHEMA.

We report for the first time (to the best of our knowledge) large increases in T_g as a result of VPI-treatment. Increasing T_g via increasing alumina content strongly supports the theory that these copolymers are becoming crosslinked. We therefore encourage further consideration of VPI as an alternative crosslinking technique. This treatment is unique compared to other curing methods in that it can be applied as a post-processing step to some products in their final form. Due to the limited diffusivity of metalorganic compounds through reactive bulk polymers, VPI crosslinking may be limited to nanoscale materials. Nonetheless, increasing T_g via VPI processing can effectively raise the maximum operating temperature of polymers such as thin films in electronic devices and nanofibers in biomedical technologies.

References

- (1) Bandzierz, K.; Reuvekamp, L.; Dryzek, J.; Dierkes, W.; Blume, A.; Bielinski, D. Influence of Network Structure on Glass Transition Temperature of Elastomers. *Materials (Basel)* **2016**, *9* (7), 607.
- (2) DiMarzio, E. A. On the Second-Order Transition of a Rubber. *J. Res. Natl. Bur. Stand. A Phys. Chem.* **1964**, *68A* (6), 611–617.
- (3) Gregorczyk, K. E.; Pickup, D. F.; Sanz, M. G.; Irakulis, I. A.; Rogero, C.; Knez, M. Tuning the Tensile Strength of Cellulose through Vapor-Phase Metalation. *Chem. Mater.* **2015**, *27* (1), 181–188.
- (4) Hanemann, T.; Szabó, D. V. Polymer-Nanoparticle Composites: From Synthesis to Modern Applications. *Materials (Basel)* **2010**, *3* (6), 3468–3517.
- (5) Hill, G. T.; Lee, D. T.; Williams, P. S.; Needham, C. D.; Dandley, E. C.; Oldham, C. J.; Parsons, G. N. Insight on the Sequential Vapor Infiltration Mechanisms of Trimethylaluminum with Poly(Methyl Methacrylate), Poly(Vinylpyrrolidone), and Poly(Acrylic Acid). *J. Phys. Chem. C Nanomater. Interfaces* **2019**, *123* (26), 16146–16152.
- (6) Jin, K.; Torkelson, J. M. Enhanced T_g-Confinement Effect in Cross-Linked Polystyrene Compared to Its Linear Precursor: Roles of Fragility and Chain Architecture. *Macromolecules* **2016**, *49* (14), 5092–5103.
- (7) Leng, C. Z.; Losego, M. D. Vapor Phase Infiltration (VPI) for Transforming Polymers into Organic–Inorganic Hybrid Materials: A Critical Review of Current Progress and Future Challenges. *Mater. Horiz.* **2017**, *4* (5), 747–771.

- (8) Kim, S.; Hewlett, S. A.; Roth, C. B.; Torkelson, J. M. Confinement Effects on Glass Transition Temperature, Transition Breadth, and Expansivity: Comparison of Ellipsometry and Fluorescence Measurements on Polystyrene Films. *Eur. Phys. J. E Soft Matter* **2009**, *30* (1), 83–92.
- (9) E.K. McGuinness, C. Leng, M.D. Losego. Increased Chemical Stability of Vapor Phase Infiltrated AlO_x-Poly(Methyl Methacrylate) Hybrid Materials. *ACS Applied Polymer Materials* **2020**. <https://doi.org/10.1021/acsapm.9b01207>.
- (10) Olmos, D.; Martín, E. V.; González-Benito, J. New Molecular-Scale Information on Polystyrene Dynamics in PS and PS-BaTiO₃ Composites from FTIR Spectroscopy. *Phys. Chem. Chem. Phys.* **2014**, *16* (44), 24339–24349.
- (11) Petkov, V.; Ren, Y.; Kabekkodu, S.; Murphy, D. Atomic Pair Distribution Functions Analysis of Disordered Low-Z Materials. *Phys. Chem. Chem. Phys.* **2013**, *15* (22), 8544–8554.
- (12) Stutz, H.; Illers, K.-H.; Mertes, J. A Generalized Theory for the Glass Transition Temperature of Crosslinked and Uncrosslinked Polymers. *J. Polym. Sci. B Polym. Phys.* **1990**, *28* (9), 1483–1498.
- (13) Waldman, R. Z.; Mandia, D. J.; Yanguas-Gil, A.; Martinson, A. B. F.; Elam, J. W.; Darling, S. B. The Chemical Physics of Sequential Infiltration Synthesis—A Thermodynamic and Kinetic Perspective. *J. Chem. Phys.* **2019**, *151* (19), 190901.
- (14) Xu, H.; Kuo, S.-W.; Lee, J.-S.; Chang, F.-C. Preparations, Thermal Properties, and T_g Increase Mechanism of Inorganic/Organic Hybrid Polymers Based on Polyhedral Oligomeric Silsesquioxanes. *Macromolecules* **2002**, *35* (23), 8788–8793.

- (15) Yang, F.; Brede, J.; Ablat, H.; Abadia, M.; Zhang, L.; Rogero, C.; Elliott, S. D.; Knez, M. Reversible and Irreversible Reactions of Trimethylaluminum with Common Organic Functional Groups as a Model for Molecular Layer Deposition and Vapor Phase Infiltration. *Adv. Mater. Interfaces* **2017**, *4* (18), 1700237.
- (16) Barry, E.; Mane, A. U.; Libera, J. A.; Elam, J. W.; Darling, S. B. Advanced Oil Sorbents Using Sequential Infiltration Synthesis. *J. Mater. Chem. A Mater. Energy Sustain.* **2017**, *5* (6), 2929–2935.
- (17) Deckman, I.; Moshonov, M.; Obuchovsky, S.; Brener, R.; Frey, G. L. Spontaneous Interlayer Formation in OPVs by Additive Migration Due to Additive–Metal Interactions. *J. Mater. Chem. A Mater. Energy Sustain.* **2014**, *2* (39), 16746–16754.
- (18) Tseng, Y.-C.; Peng, Q.; Ocola, L. E.; Czaplewski, D. A.; Elam, J. W.; Darling, S. B. Etch Properties of Resists Modified by Sequential Infiltration Synthesis. *J. Vac. Sci. Technol. B Nanotechnol. Microelectron.* **2011**, *29* (6), 06FG01.
- (19) Berman, D.; Guha, S.; Lee, B.; Elam, J. W.; Darling, S. B.; Shevchenko, E. V. Sequential Infiltration Synthesis for the Design of Low Refractive Index Surface Coatings with Controllable Thickness. *ACS Nano* **2017**, *11* (3), 2521–2530.
- (20) McGuinness, E. K.; Zhang, F.; Ma, Y.; Lively, R. P.; Losego, M. D. Vapor Phase Infiltration of Metal Oxides into Nanoporous Polymers for Organic Solvent Separation Membranes. *Chem. Mater.* **2019**, *31* (15), 5509–5518.
- (21) DeCoster, M. E.; Meyer, K. E.; Piercy, B. D.; Gaskins, J. T.; Donovan, B. F.; Giri, A.; Strnad, N. A.; Potrepka, D. M.; Wilson, A. A.; Losego, M. D.; Hopkins, P. E. Density and Size Effects

- on the Thermal Conductivity of Atomic Layer Deposited TiO₂ and Al₂O₃ Thin Films. *Thin Solid Films* **2018**, *650*, 71–77.
- (22) Sultanova, N.; Kasarova, S.; Nikolov, I. Dispersion Properties of Optical Polymers. *Acta Phys. Pol. A*. **2009**, *116* (4), 585–587.
- (23) Karaman, M.; Kooi, S. E.; Gleason, K. K. Vapor Deposition of Hybrid Organic–Inorganic Dielectric Bragg Mirrors Having Rapid and Reversibly Tunable Optical Reflectance. *Chem. Mater.* **2008**, *20* (6), 2262–2267.
- (24) Nayar, P.; Khanna, A.; Kabiraj, D.; Abhilash, S. R.; Beake, B. D.; Losset, Y.; Chen, B. Structural, Optical and Mechanical Properties of Amorphous and Crystalline Alumina Thin Films. *Thin Solid Films* **2014**, *568*, 19–24.

Appendix

